



Cite this: *Chem. Sci.*, 2021, **12**, 1479

All publication charges for this article have been paid for by the Royal Society of Chemistry

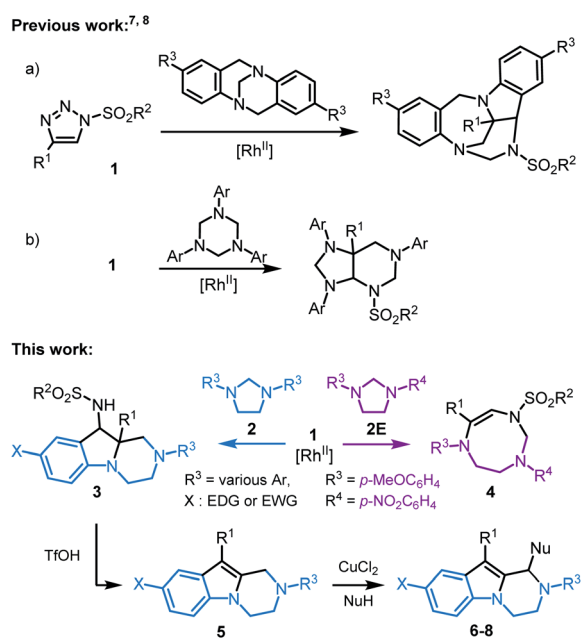
Received 16th October 2020
Accepted 21st November 2020

DOI: 10.1039/d0sc05725h
rsc.li/chemical-science

Introduction

N-Sulfonyl-1,2,3-triazoles **1**, readily accessible through Cu(1)-catalyzed azide alkyne cycloadditions (CuAACs),¹ are key building blocks in synthetic, biological and medicinal chemistry.² For the purpose of this study, they also decompose under metal-catalyzed conditions to afford α -imino carbenes.³ These electrophilic unsaturated intermediates have received much attention in recent years, as many synthetically useful and original processes can be afforded, from migrations to ylide-forming reactions and subsequent transformations.^{4,5} Only few studies have been reported on the reactivity of α -imino carbenes with tertiary amines or aminals, and on the subsequent ammonium ylide chemistry.⁶ Of special interest to the current study, Tröger bases were shown to react and yield polycyclic indoline-benzodiazepines through a cascade of [1,2]-Stevens, Friedel-Crafts, Grob and aminal formation reactions (Scheme 1, top, a).⁷ Also, 1,3,5-triazinanes form octahydro-1H-purine derivatives *via* formal [6 + 3] cycloaddition, ring-closure and rearrangements (Scheme 1, top, b).⁸ Herein, in a new development, the intermolecular reactivity of *N*-sulfonyl-1,2,3-

triazoles **1** with imidazolidines **2** is reported (Scheme 1, bottom). Under dirhodium catalysis (3 mol%), hexahydropyrazino[1,2-*a*]indoles **3** are obtained in good yields (up to 90%, diastereomeric ratio (dr) up to 6.8 : 1). Mechanistically, after the initial addition of α -imino carbenes to **2** and subsequent ylide formation, the transformation involves [1,2]-Stevens and Friedel-Crafts reactions. The process is general and yields systematically the polycyclic pyrazino-indolines **3**. However, and



Scheme 1 Reactivity of *N*-sulfonyl triazoles with aminals.

^aDepartment of Organic Chemistry, University of Geneva, Quai Ernest Ansermet 30, 1211 Geneva 4, Switzerland. E-mail: Amalia.PobladorBahamonde@unige.ch; Jerome.Lacour@unige.ch

^bLaboratory of Crystallography, University of Geneva, Quai Ernest Ansermet 24, 1211 Geneva 4, Switzerland

† The dataset for this article can be found at the following DOI: 10.26037/yareta:u5rrhlxqyrgbpijtuhqyq1eq. It will be preserved for 10 years.

‡ Electronic supplementary information (ESI) available: Synthetic protocols, $^1\text{H}/^{13}\text{C}$ NMR and HR mass spectra. CCDC 2015200–2015204. For ESI and crystallographic data in CIF or other electronic format see DOI: 10.1039/d0sc05725h



importantly, with unsymmetrically substituted imidazolidine **2E** ($R^3 = p\text{-MeOC}_6\text{H}_4$ and $R^4 = p\text{-NO}_2\text{C}_6\text{H}_4$), a regiodivergent pathway is obtained favoring the selective formation of 8-membered ring hexahydro-1,3,6-triazocines **4**.

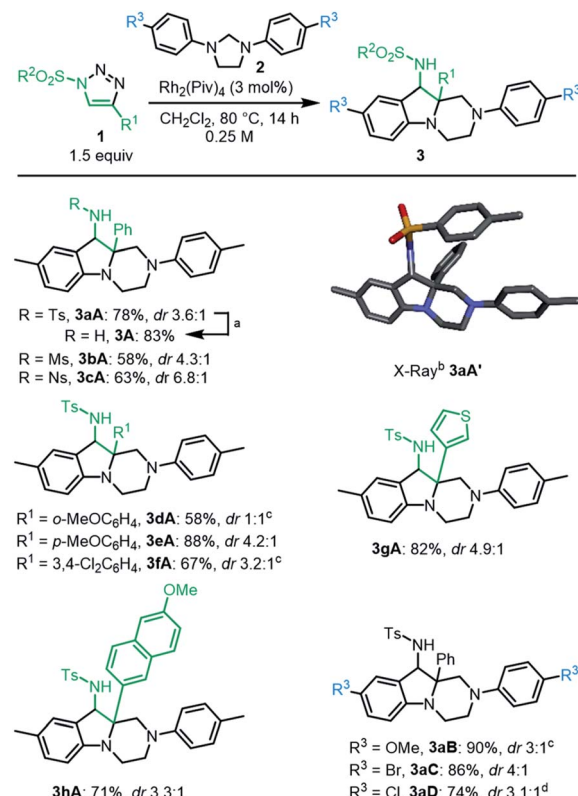
Based on first principles, detailed mechanistic analysis will show that, after regioselective ylide formation and aminal ring opening, N-cyclization rather than C-cyclization occurs in this case to form the medium sized heterocycle **4**. The influence of kinetic and thermodynamic preferences, and the occurrence of a Curtin–Hammett type situation in most cases, will be demonstrated and discussed. Furthermore, compounds **3** can be transformed into tetrahydropyrazino[1,2-*a*]indoles **5** and further derivatives **6–8** by oxidative C–C bond forming reactions. Such compounds **3**, **5–8** ought to interest medicinal chemists as pyrazino[1,2-*a*]indoles are commonly found in biologically active compounds with 5-HT_{2C} receptor agonist,⁹ antifungal,¹⁰ antibacterial,¹¹ anticancer,¹² and antiviral activities,¹³ among others (Fig. 1).¹⁴

Results and discussion

Initial experiments were performed by mixing *N*-tosyl-4-phenyl-1,2,3-triazole **1a** (1.5 equiv.), 1,3-di-*p*-tolylimidazolidine **2A** (1 equiv.) and $\text{Rh}_2(\text{Piv})_4$ (1 mol%) in CHCl_3 (0.25 M), and heating the mixture at 80 °C during 63 h. ¹H-NMR spectroscopic analysis of the crude reaction mixture revealed the presence of unreacted starting materials and two new diastereomeric products **3aA'** and **3aA''** (24% and 20% yields respectively). Their structures were determined with certainty, and the relative configuration relationship in particular, only after X-ray diffraction analysis (Scheme 1 and ESI†).

With this result in hand, optimization studies were conducted to improve the synthesis of **3aA** and results are reported in the ESI.‡ Best conditions involve the use of CH_2Cl_2 as solvent and 3 mol% of $\text{Rh}_2(\text{Piv})_4$ as catalyst.¹⁵ Complete consumption of **2A** is then achieved after 14 h at 80 °C with only a slight excess of **1a** (1.5 equiv., 0.25 M). Diastereomeric products **3aA'** and **3aA''** are then formed in 61% and 17% yields respectively. Treatment of **3aA'** with sodium (Na) and naphthalene in THF led to a complete conversion and afforded free amino **3A** in 83% yield (Scheme 2, top). A 1 mmol scale reaction was also performed affording products **3aA** with comparable yield and diastereoselectivity (77%, dr 3.6 : 1).¹⁶

With the optimized conditions in hand, a series of *N*-sulfonyl-1,2,3-triazoles **1a–1h** was prepared by CuAAC¹⁷ and tested with imidazolidines **2A–2D** (Scheme 2). Mesyl **1b** and nosyl **1c** triazoles afforded products **3bA** and **3cA** in moderate yields and diastereoselectivity (dr up to 6.8 : 1). Triazole



Scheme 2 Hexahydropyrazino[1,2-*a*]indoles **3**. ^aFrom **3aA'**: Na, naphthalene, THF, 17 h, –78 °C to 25 °C. ^bStick view of the crystal structure of **3aA'** (major diastereoisomer). ^cInseparable mixture of diastereoisomers. ^d3 equiv. of *N*-sulfonyl-1,2,3-triazole were used.

reagents **1d** to **1f** with electron donating (EDG) or electron withdrawing (EWG) groups at regiosomeric positions on aromatic group R^1 led to the corresponding heterocycles **3dA**–**3fA** in average to excellent yields (58–88%), but poor to moderate diastereoselectivity. Thiophene derived **1g** and 6-methoxynaphthalene **1h** were also compatible leading to the expected products **3gA** and **3hA** in 82% and 71% yields, respectively.

A series of imidazolidines were prepared following reported procedures¹⁸ and tested with *N*-tosyl-triazole **1a** (Scheme 2). These symmetrical substrates containing EDGs or EWGs at R^3 positions led to **3aB**–**3aD** with very good yields (74–90%) and moderate levels of diastereoselectivity.

To get some insight on the mechanism of this transformation, unsymmetrically substituted **2E** was synthesized, with electron-withdrawing *p*-NO₂ and -donating *p*-OMe substituents on the aromatic rings of the imidazolidine. Compound **2E** was then treated with *N*-tosyl triazole **1a** and $\text{Rh}_2(\text{Piv})_4$ under the optimized conditions. Careful analysis by NMR spectroscopy revealed the presence of a major product as a single regiosomer (57%). This compound was however not the expected hexahydropyrazino[1,2-*a*]indole **3aE** but 8-membered triazocine **4aE**. Interestingly and importantly for further mechanistic discussions, compounds **4aE** contains an aminal $-\text{NCH}_2\text{N}-$ bridge that is formed with the nitrogen atom

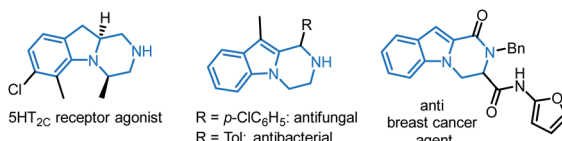


Fig. 1 Selected biologically active pyrazino[1,2-*a*]indoles.^{9b,10,11,12b}



carrying the *p*-NO₂C₆H₄ ring. The structure of **4aE** was confirmed later by X-ray diffraction analysis (Scheme 3, top). Treatment of **2E** with triazoles **1e** and **1i** also led to hexahydro-1,3,6-triazocines **4eE** and **4iE** in 56% and 36% yield, respectively. As mentioned above, these results are important to understand the reactivity pathways involved in this Rh(n)-catalyzed α -imino diazo decomposition and subsequent nitrogen ylide/cyclization processes.

Theoretical study

To rationalize the above substrate-dependent synthetic divergence toward either pyrazino-indole or triazocine products, DFT calculations were performed using the α -imino carbene complex **A** as starting point. Geometrically, in relation with the imidazolidine skeleton, the Rh-carbene faces either the aminal bridge or the -CH₂CH₂- backbone of the 5-membered ring. Both approximation modes were studied and only the most favored path is detailed here (Fig. 2 and S8[‡]). From complex **A**, the computed transition state **TS A-B** involves the C–N bond formation between the carbene complex and the imidazolidine substrate ($\Delta G^\ddagger = 7.7$ kcal mol⁻¹), achieving the nitrogen ylide **B**. The system rapidly evolves to **B'** by switching the Rh catalyst from the C to the N atom of the former α -imino carbene, in an exergonic step of 2.7 kcal mol⁻¹. In this disposition, the aminal opening occurs through **TS B'-C** with a low activation barrier ($\Delta G^\ddagger = 2.2$ kcal mol⁻¹) leading to the iminium intermediate **C** with a relative energy of 13.1 kcal mol⁻¹ below the initial reactants (full details in Fig. S1[‡]). The computed results for the donor OMe – acceptor NO₂ system (**2E**) show the same two-step process although in this case the aminal opening requires higher activation energy ($\Delta G^\ddagger = 7.2$ kcal mol⁻¹) and the final iminium intermediate **C**_{(OMe-NO₂) is stabilized by only 3.7 kcal mol⁻¹ (see further details in Fig. S4[‡]).}

At this stage, intermediate **C** can evolve either towards N- or C-cyclizations. Pathway A (Fig. 3, left) depicts the progression of intermediate **C** through an N-cyclization process, **TS C-4**, in

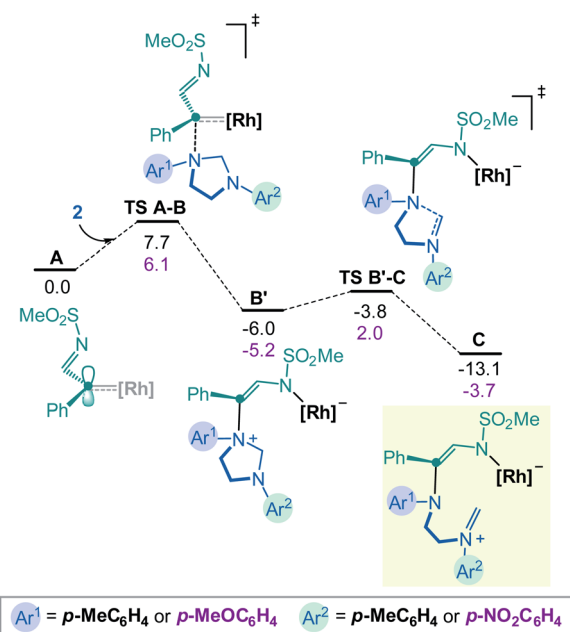


Fig. 2 Computed Gibbs energy profile for the formation of the iminium intermediate **C**. Donor–donor energies (Ar¹, Ar² EDGs) in black and donor–acceptor (Ar¹ EDG, Ar² EWG) in magenta, all in kcal mol⁻¹.

a quasi-barrier less step ($\Delta G^\ddagger = 1.3$ kcal mol⁻¹) affording the formation of the 8-membered-[Rh] complex. The Rh catalyst is then released and hexahydro-1,3,6-triazocine product **4** is formed in an exergonic reversible manner ($\Delta G = 11.7$ kcal mol⁻¹ below **C**). The C-cyclization reaction is shown in Pathway B (Fig. 3, right). First, via **TS C-D'**, the 6-membered-[Rh] complex **D'** is formed with an activation barrier of

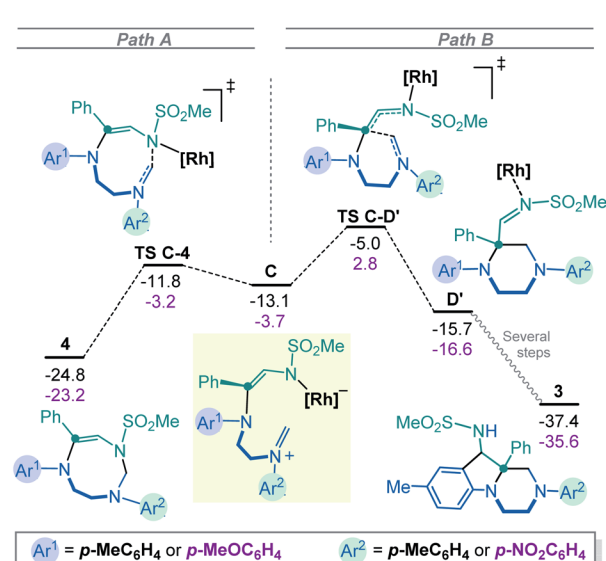
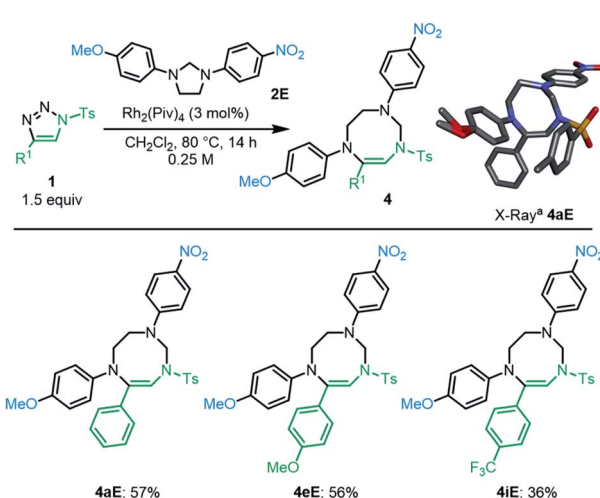


Fig. 3 Computed Gibbs energy profile for the 8-membered (left, N-cyclization) or 6-membered (right, C-cyclization) ring formation from the iminium intermediate **C**. Donor–donor (Ar¹, Ar² EDGs) energies in black and donor–acceptor (Ar¹ EDG, Ar² EWG) in magenta, all in kcal mol⁻¹.



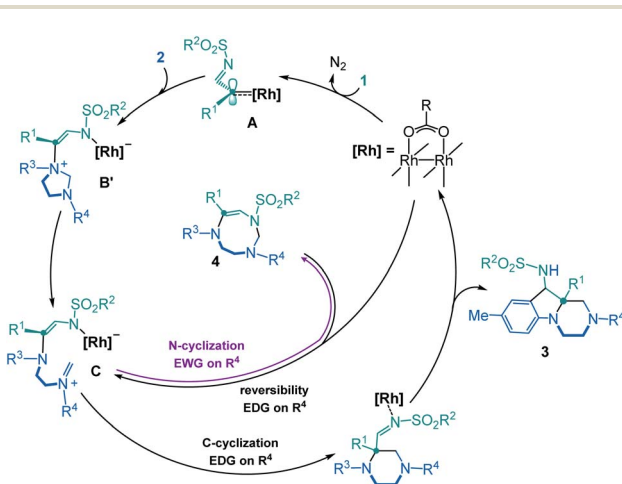
Scheme 3 Access to substituted hexahydro-1,3,6-triazocines **4**. ^aStick view of the crystal structure of **4aE**. Hydrogen atoms are omitted for clarity and the MeO group presents a local disorder.



8.1 kcal mol⁻¹. This transition state involves the bond formation between the C atom of the iminium ion and the C atom of the former carbene. It is worth to mention that the process described from **B** to **D'** corresponds to a formal [1,2]-Stevens rearrangement.¹⁹ Finally, to proceed towards the formation of hexahdropyrazino[1,2-*a*]indole **3**, intermediate **D** evolves through a Friedel-Crafts cyclization with the assistance of the Rh₂(Piv)₄ catalyst (see details in Fig. S3‡). These final steps require an overall activation energy close to 20 kcal mol⁻¹ and lead to the formation of the most stable product **3** with a relative energy of 37.4 kcal mol⁻¹ below the initial reactants. The analysis of the full reaction path follows a clear Curtin–Hammett behavior. Compound **4**, the kinetically-preferred product formed *via* **TS C-4**, can reopen in the reaction conditions again and, *via* **TS C-D'** ($\Delta G^\ddagger = 19.8$ kcal mol⁻¹), the formation of the thermodynamic product **3** is then favored. This last step is irreversible as 32.4 kcal mol⁻¹ are required to overcome **TS C-D'** from **3**.

Fig. 3 also depicts the energies for the donor–acceptor system (Ar¹ EDG, Ar² EWG, numerical values in magenta). Interestingly, in this case, **TS C-D'**_(OMe-NO₂)²⁰ has an energy of 2.8 kcal mol⁻¹ above the initial reactants which is sufficient to suppress the Curtin–Hammett behavior. In fact, once product **4** is formed, the reversibility of the opening reaction is no longer feasible. The formation of product **3** would require *ca.* 26 kcal mol⁻¹, which is not permitted in the reaction conditions. The selectivity of the carbene towards the different N atoms was also calculated when unsymmetrically substituted imidazolidine **2E** is used as substrate. The results show that the attack on the N-atom bearing the *p*-MeOC₆H₄ group is favored, in agreement with the experimental observations (see details in Fig. S12‡).

Overall, thanks to the DFT calculations that are summarized in Scheme 4, an elaborate Curtin–Hammett behavior is evidenced with derivatives **3** and **4** as the thermodynamically- and kinetically-preferred products, respectively. With symmetrical imidazolidines as substrates (Ar¹ = Ar² EDGs or weakly EWGs), the corresponding 8-membered ring derivatives of type **4** are

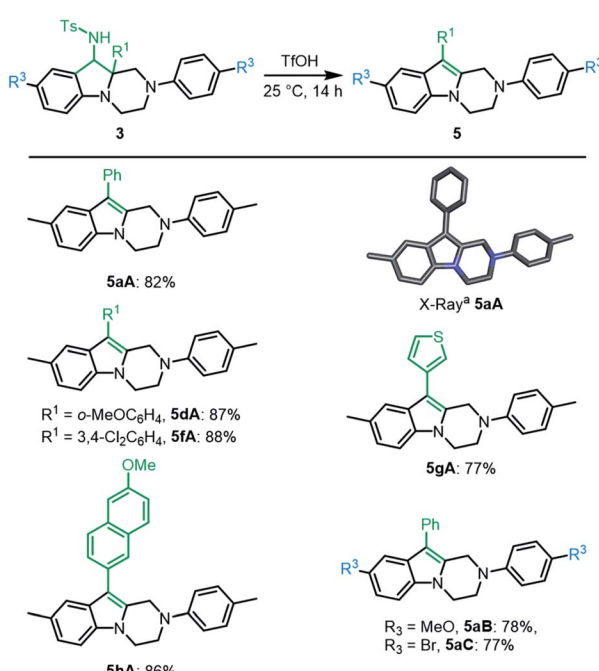


Scheme 4 Global mechanistic rationale.

unstable in the reaction conditions and evolve towards hexahdropyrazino[1,2-*a*]indoles **3**, after a reversible ring opening. Such a behavior does not occur anymore when donor–acceptor **2E** is used as reactant (Ar¹ strong EDG, Ar² strong EWG). This substrate-dependent reactivity is controlled by **TS C-D'**, the transition state at the origin of the synthetic divergence.

Extension

Finally, with hexahdropyrazino[1,2-*a*]indoles **3** in hand, care was taken to extend the chemistry to further heterocycles and addition derivatives. First, treatment of **3aA** (dr 3.6 : 1) with concentrated triflic acid (25 °C, 14 h) led to further derivatization. In fact, ¹H-NMR analysis of the crude reaction mixture revealed a full conversion and the formation of single product **5aA**, which was easily isolated in good yield (82%). Its exact structure was determined by X-ray diffraction analysis (Scheme 5, bottom). Such 1,2,3,4-tetrahydropyrazino[1,2-*a*]indole of type **5** is probably formed through protonation and elimination of TsNH₂ followed by a 1,2-shift of the aryl group (R¹) and a final proton loss (see Scheme S2‡). Isolated single diastereoisomers **3aA'** and **3aA''** were treated independently with TfOH under the reaction conditions. Product **5aA** was formed in both instances and isolated with the same yield. A series of derivatives **3A** was treated under these reaction conditions. Both electron donating and electron withdrawing substituents on the migrating phenyl group (R¹) afforded the corresponding products **5dA** and **5fA** in very good yields (87% and 88%, respectively). Other substituents R¹ such as thiophene **3gA** and 6-methoxynaphthalene **3hA** were also compatible leading to the expected products **5gA** and **5hA** in 77% and 86% yields, respectively. *p*-MeO and *p*-Br



Scheme 5 One-step access to tetrahydropyrazino[1,2-*a*]indoles **5**. ^aStick view of the crystal structure of **5aA**. Hydrogen atoms are omitted for clarity.



substituents at R³ position led to **5aB** and **5aC** in 78% and 77% yields.

Then, compounds **5** were further functionalized *via* oxidative C–C bond forming reactions using conditions similar to that reported for tetrahydroisoquinolines.²¹ In fact, treatment of **5aA** with one equivalent of CuCl₂ in THF/MeNO₂ (1 : 1) led to the corresponding iminium intermediate,^{22,23} which upon addition of Hünig's base (iPr₂EtN, 1.1 equiv.) led to the clean formation of **6** (92% yield) by an *in situ* aza-Henry reaction (Scheme 6). Further oxidative derivatizations of **5aA** were possible with silyl ketene acetals and cyanide anion as nucleophiles to afford the corresponding ester **7** and nitrile **8** in 73% and 93% yields, respectively.

Conclusions

In summary, novel hexahydropyrazinoindoles **3** were prepared in a single step from *N*-sulfonyl triazoles **1** and imidazolidines **2**. Under dirhodium catalysis, α -imino carbenes were generated and formed nitrogen ylide intermediates that, after subsequent aminal opening, afforded derivatives **3** predominantly *via* a formal C-reactivity/[1,2]-Stevens pathway and tandem Friedel–Crafts cyclization. Of mechanistic importance, a regiodivergent reactivity could be engineered through the use of unsymmetrically substituted imidazolidine substrate **2E** that promoted the exclusive formation of 8-membered ring derivative **4**. Importantly, DFT computed results demonstrated a mechanistic Curtin–Hammett-like situation. First, compounds of type **4** are formed as kinetic products and reopened reversibly with the aid of the Rh₂(Piv)₄ catalyst. Given time and energy, the system evolves towards the formation of the thermodynamically preferred product **3**, after an irreversible Friedel–Crafts alkylation that seals the multi-step pathway. With imidazolidine **2E** as reagent, the formation of **4** becomes irreversible and the 8-

membered heterocycle is formed preferentially as a unique regiosomer. Finally, with derivatives **3** in hand, tetrahydropyrazinoindoles **5** were prepared efficiently upon treatment with triflic acid; compounds **5** being themselves suitable for late-stage functionalization *via* oxidative C–C bond forming reactions giving products **6** to **8**.

Conflicts of interest

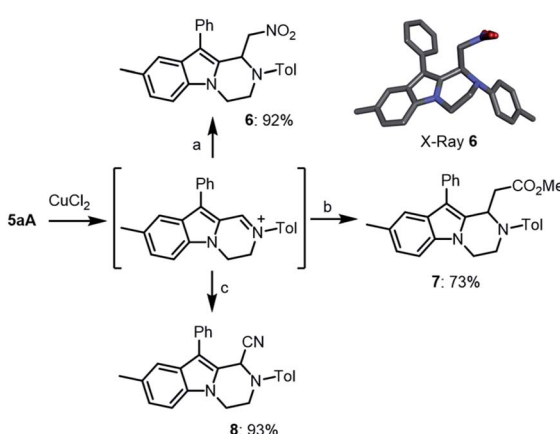
There are no conflicts to declare.

Acknowledgements

We thank the University of Geneva and the Swiss National Science Foundation for financial support (JL: 200020-172497 and 200020-184843). We also acknowledge the contributions of the Sciences Mass Spectrometry (SMS) platform at the Faculty of Sciences, University of Geneva. We also thank Carmine Chiancone for technical support.

Notes and references

- (a) M. Meldal and C. W. Tornøe, *Chem. Rev.*, 2008, **108**, 2952–3015; (b) J. E. Hein and V. V. Fokin, *Chem. Soc. Rev.*, 2010, **39**, 1302–1315; (c) B. Schulze and U. S. Schubert, *Chem. Soc. Rev.*, 2014, **43**, 2522–2571; (d) V. K. Tiwari, B. B. Mishra, K. B. Mishra, N. Mishra, A. S. Singh and X. Chen, *Chem. Rev.*, 2016, **116**, 3086–3240; (e) M. M. Haugland, S. Borsley, D. F. Cairns-Gibson, A. Elmi and S. L. Cockroft, *ACS Nano*, 2019, **13**, 4101–4110.
- (a) H. C. Kolb, M. G. Finn and K. B. Sharpless, *Angew. Chem., Int. Ed.*, 2001, **40**, 2004–2021; (b) W. G. Lewis, L. G. Green, F. Grynszpan, Z. Radić, P. R. Carlier, P. Taylor, M. G. Finn and K. B. Sharpless, *Angew. Chem., Int. Ed.*, 2002, **41**, 1053–1057; (c) F. Amblard, J. H. Cho and R. F. Schinazi, *Chem. Rev.*, 2009, **109**, 4207–4220; (d) C. Le Droumaguet, C. Wang and Q. Wang, *Chem. Soc. Rev.*, 2010, **39**, 1233–1239; (e) P. Thirumurugan, D. Matosiuk and K. Jozwiak, *Chem. Rev.*, 2013, **113**, 4905–4979.
- (a) P. Grünanger, P. V. Finzi and C. Scotti, *Chem. Ber.*, 1965, **98**, 623–628; (b) M. E. Hermes and F. D. Marsh, *J. Am. Chem. Soc.*, 1967, **89**, 4760–4764; (c) R. E. Harmon, F. Stanley, S. K. Gupta and J. Johnson, *J. Org. Chem.*, 1970, **35**, 3444–3448; (d) R. E. Harmon, R. A. Earl and S. K. Gupta, *J. Chem. Soc. D*, 1971, 296–297.
- (a) B. Chattopadhyay and V. Gevorgyan, *Angew. Chem., Int. Ed.*, 2012, **51**, 862–872; (b) A. V. Gulevich and V. Gevorgyan, *Angew. Chem., Int. Ed.*, 2013, **52**, 1371–1373; (c) H. M. Davies and J. S. Alford, *Chem. Soc. Rev.*, 2014, **43**, 5151–5162; (d) P. Anbarasan, D. Yadagiri and S. Rajasekar, *Synthesis*, 2014, **46**, 3004–3023; (e) Y. Wang, X. Lei and Y. Tang, *Synlett*, 2015, **26**, 2051–2059; (f) Y. Jiang, R. Sun, X.-Y. Tang and M. Shi, *Chem.-Eur. J.*, 2016, **22**, 17910–17924.
- (a) S. Chuprakov, F. W. Hwang and V. Gevorgyan, *Angew. Chem., Int. Ed.*, 2007, **46**, 4757–4759; (b) S. Chuprakov, S. W. Kwok, L. Zhang, L. Lercher and V. V. Fokin, *J. Am. Chem. Soc.*, 2009, **131**, 18034–18035; (c) S. Chuprakov,



Scheme 6 Late stage functionalization of **5aA** *via* oxidative C–C bond formation: (a) (i) CuCl₂ (1 equiv.), THF/MeNO₂ (1 : 1), 25 °C, 3 h; (ii) iPr₂EtN (1.1 equiv.), 25 °C, 2 h. (b) (i) CuCl₂ (1 equiv.), THF, 25 °C, 16 h; (ii) 1-(tert-butyldimethylsilyloxy)-1-methoxyethene (2 + 1 equiv.), 25 °C, 6 h. (c) CuCl₂ (1 equiv.), THF, 25 °C, 16 h; (ii) NaCN (1.5 + 1.5 equiv.), MeOH, 25 °C, 6 h. Insert: stick view of the crystal structure of **6**. Hydrogen atoms are omitted for clarity and the CH₂NO₂ chain presents a local disorder.



J. A. Malik, M. Zibinsky and V. V. Fokin, *J. Am. Chem. Soc.*, 2011, **133**, 10352–10355; (d) M. Zibinsky and V. V. Fokin, *Org. Lett.*, 2011, **13**, 4870–4872; (e) D. Yadagiri and P. Anbarasan, *Chem.-Eur. J.*, 2013, **19**, 15115–15119; (f) E. E. Schultz and R. Sarpong, *J. Am. Chem. Soc.*, 2013, **135**, 4696–4699; (g) T. Miura, T. Tanaka, K. Matsumoto and M. Murakami, *Chem.-Eur. J.*, 2014, **20**, 16078–16082; (h) T. Miura, T. Nakamuro, C.-J. Liang and M. Murakami, *J. Am. Chem. Soc.*, 2014, **136**, 15905–15908; (i) D. Yadagiri and P. Anbarasan, *Org. Lett.*, 2014, **16**, 2510–2513; (j) F. Medina, C. Besnard and J. Lacour, *Org. Lett.*, 2014, **16**, 3232–3235; (k) V. N. G. Lindsay, H. M. F. Viart and R. Sarpong, *J. Am. Chem. Soc.*, 2015, **137**, 8368–8371; (l) R. W. Kubiak, J. D. Mighion, S. M. Wilkerson-Hill, J. S. Alford, T. Yoshidomi and H. M. L. Davies, *Org. Lett.*, 2016, **18**, 3118–3121; (m) A. Guarnieri-Ibáñez, F. Medina, C. Besnard, S. L. Kidd, D. R. Spring and J. Lacour, *Chem. Sci.*, 2017, **8**, 5713–5720; (n) T. Miura, Q. Zhao and M. Murakami, *Angew. Chem., Int. Ed.*, 2017, **56**, 16645–16649; (o) X. Ma, X. Xie, L. Liu, R. Xia, T. Li and H. Wang, *Chem. Commun.*, 2018, **54**, 1595–1598; (p) Z. Liu, Q. Du, H. Zhai and Y. Li, *Org. Lett.*, 2018, **20**, 7514–7517; (q) Z. J. Garlets and H. M. L. Davies, *Org. Lett.*, 2018, **20**, 2168–2171; (r) R. Jia, J. Meng, J. Leng, X. Yu and W. P. Deng, *Chem.-Asian J.*, 2018, **13**, 2360–2364; (s) D. Yadagiri, M. Chaitanya, A. C. S. Reddy and P. Anbarasan, *Org. Lett.*, 2018, **20**, 3762–3765; (t) Z.-F. Xu, L. Shan, W. Zhang, M. Cen and C.-Y. Li, *Org. Chem. Front.*, 2019, **6**, 1391–1396; (u) P. B. De, S. Atta, S. Pradhan, S. Banerjee, T. A. Shah and T. Punniyamurthy, *J. Org. Chem.*, 2020, **85**, 4785–4794; (v) A. C. S. Reddy, K. Ramachandran, P. M. Reddy and P. Anbarasan, *Chem. Commun.*, 2020, **56**, 5649–5652; (w) H. J. Dequina, J. Eshon, W. T. Raskopf, I. Fernández and J. M. Schomaker, *Org. Lett.*, 2020, **22**, 3637–3641; (x) T. Miura, T. Nakamuro, Y. Ishihara, Y. Nagata and M. Murakami, *Angew. Chem., Int. Ed.*, 2020, **59**, 20475–20479.

6 (a) S. Chuprakov, S. W. Kwok and V. V. Fokin, *J. Am. Chem. Soc.*, 2013, **135**, 4652–4655; (b) H. J. Jeon, D. J. Jung, J. H. Kim, Y. Kim, J. Bouffard and S.-g. Lee, *J. Org. Chem.*, 2014, **79**, 9865–9871; (c) D. J. Lee, H. S. Han, J. Shin and E. J. Yoo, *J. Am. Chem. Soc.*, 2014, **136**, 11606–11609; (d) D. J. Lee, D. Ko and E. J. Yoo, *Angew. Chem., Int. Ed.*, 2015, **54**, 13715–13718; (e) X. Lei, L. Li, Y.-P. He and Y. Tang, *Org. Lett.*, 2015, **17**, 5224–5227; (f) H.-D. Xu, Z.-H. Jia, K. Xu, H. Zhou and M.-H. Shen, *Org. Lett.*, 2015, **17**, 66–69; (g) T. Ryu, Y. Baek and P. H. Lee, *J. Org. Chem.*, 2015, **80**, 2376–2383; (h) Y.-Z. Zhao, H.-B. Yang, X.-Y. Tang and M. Shi, *Chem.-Eur. J.*, 2015, **21**, 3562–3566; (i) Y. Wang, X. Lei and Y. Tang, *Chem. Commun.*, 2015, **51**, 4507–4510; (j) N. V. Rostovskii, J. O. Ruvinskaya, M. S. Novikov, A. F. Khlebnikov, I. A. Smetanin and A. V. Agafonova, *J. Org. Chem.*, 2017, **82**, 256–268.

7 (a) A. Bosmani, A. Guarnieri-Ibáñez, S. Goudedranche, C. Besnard and J. Lacour, *Angew. Chem., Int. Ed.*, 2018, **57**, 7151–7155; (b) A. Bosmani, A. Guarnieri-Ibáñez and J. Lacour, *Helv. Chim. Acta*, 2019, **102**, e1900021.

8 J. Ge, X. Wu and X. Bao, *Chem. Commun.*, 2019, **55**, 6090–6093.

9 (a) M. Bös, F. Jenck, J. R. Martin, J. L. Moreau, V. Mutel, A. J. Sleight and U. Widmer, *Eur. J. Med. Chem.*, 1997, **32**, 253–261; (b) S. Röver, D. R. Adams, A. Bénardeau, J. M. Bentley, M. J. Bickerdike, A. Bourson, I. A. Cliffe, P. Coassolo, J. E. P. Davidson, C. T. Dourish, P. Hebeisen, G. A. Kennett, A. R. Knight, C. S. Malcolm, P. Mattei, A. Misra, J. Mizrahi, M. Muller, R. H. P. Porter, H. Richter, S. Taylor and S. P. Vickers, *Bioorg. Med. Chem. Lett.*, 2005, **15**, 3604–3608; (c) H. G. F. Richter, D. R. Adams, A. Benardeau, M. J. Bickerdike, J. M. Bentley, T. J. Blench, I. A. Cliffe, C. Dourish, P. Hebeisen, G. A. Kennett, A. R. Knight, C. S. Malcolm, P. Mattei, A. Misra, J. Mizrahi, N. J. T. Monck, J. M. Plancher, S. Roever, J. R. A. Roffey, S. Taylor and S. P. Vickers, *Bioorg. Med. Chem. Lett.*, 2006, **16**, 1207–1211; (d) N. Krogsgaard-Larsen, A. A. Jensen and J. Kehler, *Bioorg. Med. Chem. Lett.*, 2010, **20**, 5431–5433.

10 R. K. Tiwari, A. K. Verma, A. K. Chhillar, D. Singh, J. Singh, V. Kasi Sankar, V. Yadav, G. L. Sharma and R. Chandra, *Bioorg. Med. Chem.*, 2006, **14**, 2747–2752.

11 R. K. Tiwari, D. Singh, J. Singh, V. Yadav, A. K. Pathak, R. Dabur, A. K. Chhillar, R. Singh, G. L. Sharma, R. Chandra and A. K. Verma, *Bioorg. Med. Chem. Lett.*, 2006, **16**, 413–416.

12 (a) Z. Shiokawa, K. Hashimoto, B. Saito, Y. Oguro, H. Sumi, M. Yabuki, M. Yoshimatsu, Y. Kosugi, Y. Debori, N. Morishita, D. R. Dougan, G. P. Snell, S. Yoshida and T. Ishikawa, *Bioorg. Med. Chem.*, 2013, **21**, 7938–7954; (b) Y. J. Kim, J. S. Pyo, Y.-S. Jung and J.-H. Kwak, *Bioorg. Med. Chem. Lett.*, 2017, **27**, 607–611.

13 G. Zoidis, E. Giannakopoulou, A. Stevaert, E. Frakolaki, V. Myrianthopoulos, G. Fytas, P. Mavromara, E. Mikros, R. Bartenschlager, N. Vassilaki and L. Naesens, *RSC Med. Chem.*, 2016, **7**, 447–456.

14 (a) R. A. Bit, P. D. Davis, L. H. Elliott, W. Harris, C. H. Hill, E. Keech, H. Kumar, G. Lawton, A. Maw, J. S. Nixon, D. R. Vesey, J. Wadsworth and S. E. Wilkinson, *J. Med. Chem.*, 1993, **36**, 21–29; (b) D. M. Vigushin, G. Brooke, D. Willows, R. C. Coombes and C. J. Moody, *Bioorg. Med. Chem. Lett.*, 2003, **13**, 3661–3663; (c) D. R. Goldberg, Y. Choi, D. Cogan, M. Corson, R. DeLeon, A. Gao, L. Gruenbaum, M. H. Hao, D. Joseph, M. A. Kashem, C. Miller, N. Moss, M. R. Netherton, C. P. Pargellis, J. Pelletier, R. Sellati, D. Skow, C. Torcellini, Y. C. Tseng, J. Wang, R. Wasti, B. Werneburg, J. P. Wu and Z. Xiong, *Bioorg. Med. Chem. Lett.*, 2008, **18**, 938–941; (d) Z. Xiong, D. A. Gao, D. A. Cogan, D. R. Goldberg, M.-H. Hao, N. Moss, E. Pack, C. Pargellis, D. Skow, T. Trieselmann, B. Werneburg and A. White, *Bioorg. Med. Chem. Lett.*, 2008, **18**, 1994–1999; (e) H. G. F. Richter, C. Freichel, J. Huwyler, T. Nakagawa, M. Nettekoven, J. M. Plancher, S. Raab, O. Roche, F. Schuler, S. Taylor, C. Ullmer and R. Wiegand, *Bioorg. Med. Chem. Lett.*, 2010, **20**, 5713–5717; (f) D. J. Buzard, T. O. Schrader, X. Zhu, J. Lehmann, B. Johnson, M. Kasem, S. H. Kim, A. Kawasaki, L. Lopez, J. Moody, S. Han, Y. Gao, J. Edwards, J. Barden, J. Thatte,



J. Gatlin and R. M. Jones, *Bioorg. Med. Chem. Lett.*, 2015, **25**, 659–663.

15 With chiral catalysts such $\text{Rh}_2(R\text{-DOSP})_4$ or $\text{Rh}_2(S\text{-TCP TTL})_4$, only racemic product **3aA** is obtained. This could be an indication that a racemization of intermediate **D'** occurs *in situ*. See ref. 7b for such a possibility involving a sequence of Mannich and retro-Mannich reactions. Calculations further indicate that the barrier for the retro-Mannich is affordable in the experimental conditions (see Fig. 3).

16 Somewhat surprisingly, the Friedel–Crafts reaction leads to the preferred formation of the *cis*-adduct over the *trans*-diastereoisomer. This predominance can be rationalized *in silico* by a difference ($\Delta\Delta G^\ddagger$ 2.3 kcal mol⁻¹) between the corresponding transition states. See Fig. S13[‡] for details.

17 J. Raushel and V. V. Fokin, *Org. Lett.*, 2010, **12**, 4952–4955.

18 (a) C. H. Yoder and J. J. Zuckerman, *Inorg. Chem.*, 1967, **6**, 103–107; (b) A. R. Katritzky, W. Fan and C. Fu, *J. Org. Chem.*, 1990, **55**, 3209–3213; (c) A. J. Arduengo, R. Krafczyk, R. Schmutzler, H. A. Craig, J. R. Goerlich, W. J. Marshall and M. Unverzagt, *Tetrahedron*, 1999, **55**, 14523–14534; (d) M. K. Denk, S. Gupta, J. Brownie, S. Tajammul and A. J. Lough, *Chem.-Eur. J.*, 2001, **7**, 4477–4486.

19 R. Bach, S. Harthong and J. Lacour, in *Comprehensive Organic Synthesis II*, ed. P. Knochel, Elsevier, Amsterdam, 2nd edn, 2014, pp. 992–1037.

20 This transition state was computed as single point since full optimization led to problems with the convergence due to the intrusion of imaginary frequencies related to the methyl groups of the $\text{Rh}_2(\text{Piv})_4$ catalyst.

21 (a) D. Sureshkumar, A. Sud and M. Klussmann, *Synlett*, 2009, **10**, 1558–1561; (b) E. Boess, D. Sureshkumar, A. Sud, C. Wirtz, C. Farès and M. Klussmann, *J. Am. Chem. Soc.*, 2011, **133**, 8106–8109; (c) E. Boess, C. Schmitz and M. Klussmann, *J. Am. Chem. Soc.*, 2012, **134**, 5317–5325; (d) J. Dhineshkumar, M. Lamani, K. Alagiri and K. R. Prabhu, *Org. Lett.*, 2013, **15**, 1092–1095; (e) G. Bergonzini, C. S. Schindler, C.-J. Wallentin, E. N. Jacobsen and C. R. J. Stephenson, *Chem. Sci.*, 2014, **5**, 112–116; (f) Y. Liu, C. Wang, D. Xue, M. Xiao, C. Li and J. Xiao, *Chem.-Eur. J.*, 2017, **23**, 3051–3061; (g) G. Oss, S. D. de Vos, K. N. H. Luc, J. B. Harper and T. V. Nguyen, *J. Org. Chem.*, 2018, **83**, 1000–1010.

22 N. Saleh, A. Bosmani, C. Besnard, T. Bürgi, D. Jacquemin and J. Lacour, *Org. Lett.*, 2020, **22**, 7599–7603.

23 Synthetic attempts to isolate and characterize the *in situ* generated iminium salt were unfortunately unsuccessful.

